Available online at www.sciencedirect.com
SCIENCE DIRECT®
Thermochimica Acta 402 (2003) 159–168
thermochimica acta
www.elsevier.com/locate/tca

Dynamic heat capacity in the α relaxation process of poly(vinyl acetate) at low frequency

M. Castro*, J.A. Puértolas

Dpto. Ciencia y Tecnología de Materiales y Fluidos, Centro Politécnico Superior-ICMA, Universidad de Zaragoza-CSIC, 50018 Zaragoza, Spain

Received 29 July 2002; received in revised form 31 July 2002; accepted 28 November 2002

Abstract

The segmental relaxation in poly(vinyl acetate) (PVAC) has been studied through the determination of the isobaric dynamic heat capacity: $C_p^*(\omega, T) = C_p'(\omega, T) - iC_p''(\omega, T)$. The calorimetric measurements have been performed over a very low frequency range from 1 to 20 mHz using ac calorimetry. The real and imaginary parts of $C_p^*(\omega, T)$ at constant frequency reflect the α relaxation associated with the glass transition, but a low signal to noise ratio and/or some small unwanted contribution distorts the thermal behaviour of the imaginary component. In this work, we show that in order to estimate a suitable thermal dependence of the imaginary part an approximated method, tested before by means of dielectric relaxation spectroscopy (DRS) measurements, can be applied. A comparative analysis of the calculated effective relaxation time and the peak width has been performed with respect to the reported data, measured by both the specific heat spectroscopy (SHS) and modulated DSC (TMDSC) techniques, and DRS.

Keywords: Dynamic heat capacity; ac calorimetry; Dielectric; Relaxation; Glass transition

1. Introduction

In recent years, several studies on the dynamics of supercooled liquids and polymeric melts focus on the glass transition [1]. At temperatures above this thermodynamic event, considered as a phase transition, the structural relaxation takes place on a larger time scale that those involved in the standard techniques. The temperature dependence of the experimental relaxation time follows a non-Arrhenius behaviour and in consequence leads to a critical temperature in which the relaxation time diverges. The evaluation of the entropy variation of the supercooled liquid with respect to the crystal phase introduces the Kauzmann temperature [2], below which the entropy variation would become negative. Both temperatures are different for the assigned glass transition temperature. On the other hand, the shape of the isothermal relaxation spectra, especially in dielectric measurements [3,4] can be scaled to a master curve using the frequency of the maximum, the width, and the intensity of the relaxation. These former features have been dealt with different theories proposed in recent years [3,4] like the mode-coupling theory among others [5,6]. In this context, the availability of other relaxation techniques, would allow comparison with predictions of these theories and collate the universality of empirical scaling in the glass-forming liquid. The dynamic heat

* Corresponding author. Tel.: +34-976762528; fax: +34-976761957.
E-mail address: mcastro@posta.unizar.es (M. Castro).

0040-6031/03/$ – see front matter © 2002 Elsevier Science B.V. All rights reserved.
doi:10.1016/S0040-6031(02)00574-9

capacity, $C_p^*(\omega, T) = C_p'(\omega, T) - iC_p''(\omega, T)$, arises in systems which possess internal degrees of freedom coupled to the entropy and relaxing slowly over the time scale of the experiment. From a statistical point of view, $C_p^*(\omega)$ appears as a consequence of entropy fluctuations [7]. One advantage of the dynamic heat capacity in comparison to other techniques is the fact that $C_p^*(\omega, T)$ reflects the contribution of all modes, orientational and translational, providing global and direct information of the slow dynamics associated with the glass transition.

From an experimental point of view, the pioneering work in this field was performed by Christensen [8], using ac calorimetry over a short range of frequencies (1–30 mHz). Birge and Nagel [9], using a specific heat spectroscopy (SHS) technique, performed a study over an extended frequency range (0.1 Hz–3 kHz). Finally, a extension of the traditional DSC, named modulated DSC (TMDSC) [10], is used although there still opens problems respect to its technical and data evaluation. Different systems have been dealt with using these techniques such as supercooled liquids [8,9,11], studied by ac calorimetry and SHS, liquid crystals [12] and biological materials [13–15] by ac calorimetry and more recently polymers [16–23], in particular the poly(vinyl acetate) (PVAC) using SHS [16] and TMDSC [17].

The three techniques have some experimental difficulties which can avoid a good estimation of the imaginary part of the $C_p^*(\omega, T)$, especially when this contribution is quite small. The SHS [16,24] which shows the highest frequency range has limits on both side. At high frequencies, a considerable scatter appears due to a strong decrease of the signal to noise ratio and a significant contribution from the heater itself dominates, while at lower frequencies the influence of the finite size and geometry of the heater and sample disturbs the curve. For the TMDSC, the frequencies must be kept low enough because when the frequency increases the contribution to the phase angle due to the influence of the finite heat conductance between sample and thermometer increases and deforms the thermal behaviour of the imaginary part. Recently, a process based on the thermal dependence of the real part has been proposed in order to subtract this contribution [25]. Finally, the ac calorimetry has also a upper frequency limit due to the influence of the finite thermal conductivity and conductances which introduce new frequency-dependent terms to evaluate the dynamic heat capacity which affects principally the small imaginary part [26].

This paper has two objectives. One is to apply an approximated method, discussed in a previous paper [27], which allows to evaluate the thermal dependence of the imaginary part of the general complex susceptibility from the real contribution. In that work, a general and complete description of the method was performed and its soundness was tested by means of dielectric measurements on the PVAC polymer studying the α and β relaxations. The method has shown a acceptable agreement respect with the maximum temperature of the $\varepsilon''(T)$ and the width and shape of the loss peak between the experimental and estimated imaginary part. In this paper, we apply the method to the dynamic heat capacity on the same PVAC compound which shows a small and distorted imaginary contribution. This situation gives the opportunity to apply the method in accordance with its main purpose which is to evaluate the loss component when the experimental determination cannot resolve this contribution.

The second goal is to study the dynamics of the glass transition of polymers at very low frequencies using ac calorimetry. We have chosen PVAC for this study in order to carry out a comparative analysis with the previous SHS Beiner's data [16] and TMDSC Hensel's data [17] in this compound. The use of a different dynamic technique, in spite of its small frequency range, can provide us information in order to understand the differences between SHS and TMDSC data with respect to the effective relaxation times and the width of the loss peak. As far as we know, it is the second time [23] that measurements by ac calorimetry on polymers will be analysed and compared with other thermal dynamic techniques in the same compound, but in our case the ac calorimetric measurements have been done in the mHz low frequency range.

2. Experimental

2.1. Sample

The sample of PVAC was purchased from The Aldrich Chemical Company. The average molecular mass, M_w, is 500,000 g/mol. This value is close to of the samples used in the SHS and TMDSC

measurements [16,17]. The glass transition temperature was obtained in a conventional way from DSC measurements, using a DSC7 Perkin-Elmer calorimeter, previously calibrated in temperature and energy using standard indium and zinc samples. The heating rate was 10 K/min and the value of the half step temperature obtained was $37 \pm 2\,^{\circ}C$, after a first heating up to 100 °C and a cooling down to −10 °C were done at the same rate.

2.2. Setups and methods

The dynamic heat capacity data were obtained using an ac calorimeter suitable for measuring liquid and solid samples in the temperature range from 25 to 250 °C. This apparatus is well described elsewhere [28]. The modulated heat power was supplied by means of a strain gauge, the sensor for the temperature oscillations was a microbead thermistor, and the signal was detected by a lock-in amplifier (EG&G model 5302), which permits extension of the frequency range down to 1 mHz. The temperature is measured by a certified (MINCO) platinum thermometer which is also used to calibrate the thermistor for each measurement in order to determine the sample temperature. The encapsulated sample, 7 mg, was held at temperatures above 90 °C for 1 day under a 10^{-1} mbar pressure of helium gas, before to start the first ac calorimetric measurements. After each constant frequency measurement, the cooling of the sample is performed during several hours (around 12 h) down to room temperature.

The method for measuring $C_p^*(\omega)$ using an ac calorimeter is based on its thermal model, which can be represented by the scheme shown in Fig. 1. The sample is thermally linked to the bath by wires and helium exchange gas surrounding the capsule. This link is described by a thermal conductance, K_B. When an ac heat input, $P_{ac}\,e^{i\omega t}$, is supplied to a sample with a heat capacity, C_p, temperature oscillations are induced in the sample at the same frequency, although they are out of phase with respect to the power input. The complex amplitude T_{ac}^* [13] is given by

$$T_{ac}^* = \frac{P_{ac}}{K_B + i\omega C_p} \tag{1}$$

where the modulus of T_{ac}^* and the phase lag, denoted by T_{ac} and Φ, respectively, considering that the heat capacity would be in general complex, $C_p^*(\omega) = C_p'(\omega) - iC_p''(\omega)$, can be calculated through the following equations:

$$T_{ac} = \frac{P_{ac}}{\omega C_p'(\omega)} \left\{ 1 + \left[\frac{K_B}{\omega C_p'(\omega)} + \frac{C_p''(\omega)}{C_p'(\omega)} \right]^2 \right\}^{-1/2} \tag{2}$$

$$\Phi = -\frac{\pi}{2} + \arctan\left[\frac{K_B}{\omega C_p'(\omega)} + \frac{C_p''(\omega)}{C_p'(\omega)} \right] \tag{3}$$

where P_{ac} is the root mean square of the power. The above model and expressions have been obtained bearing in mind certain conditions. The angular frequency of the heat input, ω, and the internal relaxation time, τ_D, must fulfil the condition $\omega\tau_D \ll 1$ in order to avoid the existence of a thermal gradient in the sample. This condition limits the highest frequency which can be used in this method. The standard operating mode of an ac calorimeter involves the use of a frequency such that $\omega C_p / K_B \gg 1$. With this condition and for the case that no frequency dependence exists, we can relate the amplitude of the oscillations, T_{ac}, with the static specific heat of the sample, C_p, by the simple equation, $C_p = P_{ac}/\omega T_{ac}$.

When slow relaxating processes exist, $C_p'(\omega)$ and $C_p''(\omega)$ can be given in function of the $C_{eff} = P_{ac}/\omega T_{ac}$ and Φ experimental data by using Eqs. (2) and (3) as follows:

$$C_p'(\omega) = -C_{eff} \sin\Phi = -\frac{P_{ac}}{\omega T_{ac}} \sin\Phi \tag{4}$$

$$C_p''(\omega) = C_{eff} \cos\Phi - \frac{K_B}{\omega} = \frac{P_{ac}}{\omega T_{ac}} \cos\Phi - \frac{K_B}{\omega} \tag{5}$$

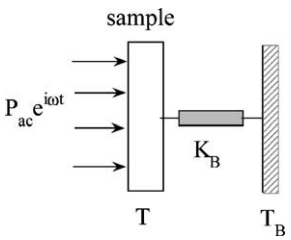

Fig. 1. Schematic thermal model for the ac calorimetry measurements.

These expressions are right even if the $\omega C_p/K_B \gg 1$ condition is not satisfied. The measurements supplied directly T_{ac} and Φ_T (total phase shift which includes the contribution from the electronic setup discussed in the results section), while ω and P_{ac} are input parameters. The values of the last parameters are established in order to be in agreement with the thermal model described before and to induce small temperature oscillations (lower than 100 mK). However, and since we also need to know the thermal conductance, K_B, additional experiments must be carried out in order to determine it. Basically, when a dc power is applied to the sample, P_0, a dc temperature step ΔT respect to the block is created and equal to P_0/K_B. From this relation K_B can be determined knowing P_0 and measuring ΔT.

Dielectric measurements were performed using a dielectric spectrometer (Novocontrol BDS4000), which included a two-terminal dielectric cell, a frequency response analyzer (Solartron 1250), and a high-impedance preamplifier of variable gain. Temperature measurement are done by means of a calibrated PT 100 temperature sensor located near the sample. The complex dielectric constant was obtained by sweeping the frequency in the range from 0.7 Hz to 1 MHz at different stabilised (±0.2 °C) temperatures. The isochronal runs were performed at a scan rate of 4 K/h. The sample was held between the condenser plates with the aid of quartz fibres and was heated to 110 °C before starting the measurements.

3. Results and discussion

3.1. Calorimetric measurements

Three consecutive heating runs at different frequencies (ν = 2, 10, 20 mHz) were performed on PVAC at a scanning rate of 1 K/h. The direct measured data are the amplitude of the temperature oscillations, T_{ac}, and the phase shift, Φ_T. Since the experimental phase, Φ_T, incorporates an electronics setup contribution, we must subtract this part to obtain only the sample contribution. Assuming that the former is temperature-independent, the correction is performed by taking for each frequency a phi value which cancels $C''_p(T)$ at a temperature far enough from the relaxation for each frequency. We have chosen 25 °C as such temperature because is far of the temperature range expected for the α relaxation and also no secondary relaxations are present. Fig. 2 shows these results for ν = 10 mHz, in the C_{eff} and Φ representation, as an example. The thermal variation of these raw data reflect the glass transition by means of a smooth step in the effective heat capacity and a broad anomaly in the phase shift. For a better comparative analysis between the different spectroscopic techniques, we have used the normalised function, $\theta^* = \theta' - i\theta''$, where

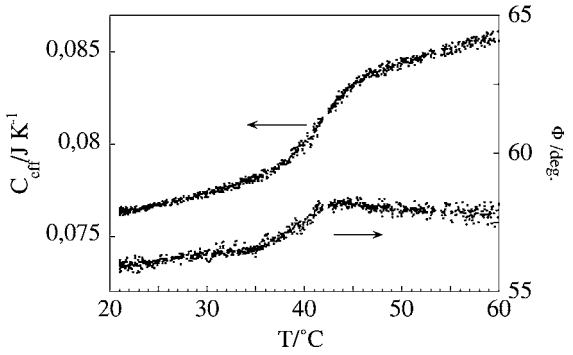

Fig. 2. Experimental ac calorimetric results for ν = 10 mHz. Both the effective heat capacity defined as $C_{eff} = P_{ac}/\omega T_{ac}$ (left scale) and the phase shift Φ between the temperature oscillation and the heating power (right scale) are shown.

$$\theta'(T) = \frac{C'_p(T) - C_{pg}(T)}{C_{pl}(T) - C_{pg}(T)} \quad (6)$$

$$\theta''(T) = \frac{C''_p(T)}{C_{pl}(T) - C_{pg}(T)} \quad (7)$$

These equations improve the definition of the half height of the step curve $C'_p(T)$, because they incorporate the thermal dependence of the specific heat out the transition for the liquid (C_{pl}) and glass (C_{pg}) states. In addition, $\theta'(T)$ will be used, as we will explain latter, to estimate the imaginary part of the dynamic heat capacity. The function, $\theta^*(T)$, has been calculated using the linear temperature dependence for $C_{pg}(T)$ and $C_{pl}(T)$ observed from regions far enough of the glass transition. The results of $\theta'(T)$ at ν = 2, 10, 20 mHz obtained with the expressions (4) and (6) together with its smooth curves are depicted in Fig. 3. A smooth step in $\theta'(T)$ in the range from 36 to 48 °C appears in all the runs, associated to the α relaxation, with a

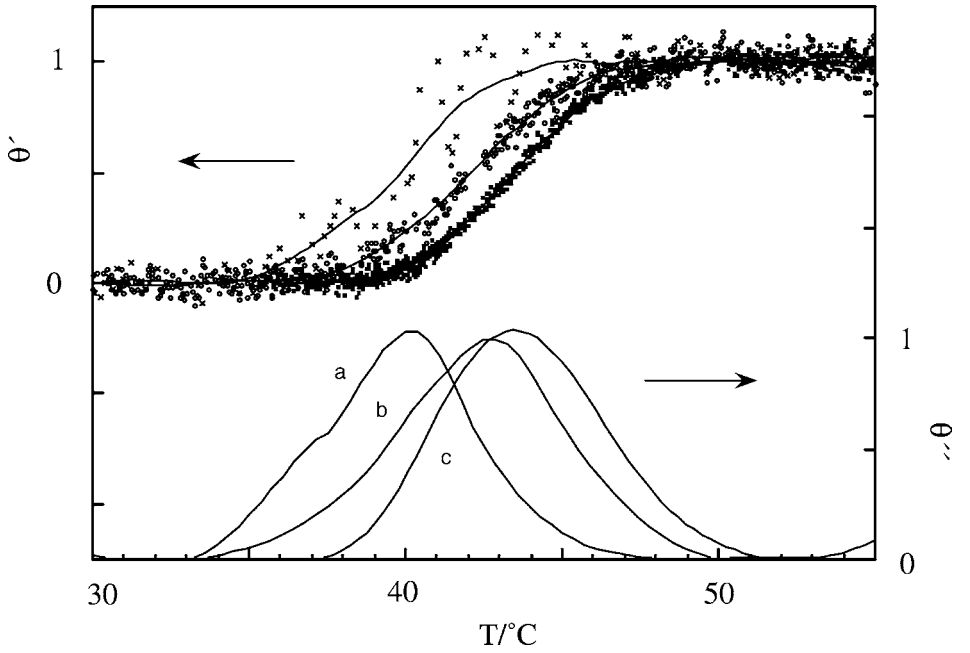

Fig. 3. Temperature dependence of the complex normalised function, $\theta^*(T)$, at different frequencies. Real part (left scale) (×) $\nu = 2$ mHz, (○) $\nu = 10$ mHz, (●) $\nu = 20$ mHz. The continuous lines are the smooth fits to the experimental points. The continuous lines at the bottom correspond to the imaginary part (right scale) of the normalised function calculated through the mathematical procedure explained in the text: (a) $\nu = 2$, (b) $\nu = 10$, and (c) $\nu = 20$ mHz.

positive shift in the frequency dependence of the half height step temperatures.

The calculation of $C''_p(T)$ by means of Eq. (5) and consequently $\theta''(T)$ is more difficult because a thermal variation of $K_B(T)$ must be known. In that sense, we have measured $K_B(T)$ ($K_B = P_0/\Delta T$) at temperatures below and above the glass transition and we have assumed a linear thermal variation around the glass transition. The results of $\theta''(T)$ present very small values compared to $\theta'(T)$ (almost two orders of magnitude) and a strong scatter due to the fact that θ'' is very sensible to the corrected phase, which shows a strong dispertion. In spite of the rough data of $\theta''(T)$, this magnitude presents an anomaly associated to the segmental process, although the unexpected shape of this peak for the highest temperatures avoids a clear determination of its maximum. A small drift of the electronics setup contribution could contribute to this effect. As consequence, we have not considered these $\theta''(T)$ experimental results in the further analysis of the α relaxation.

Alternatively, we have used a method which allows to obtain the imaginary part from the thermal variation of the real part giving for the α relaxation a good estimation of the temperature of the maximum and width of the $\theta''(T)$ peak [27]. This method has been also applied for dielectric relaxations on this same compound. Briefly, the method uses a mathematical relationship between the partial derivative of θ', T and ω, together with the assumptions that the segmental relaxation time follows a VFTH (Vogel–Fulcher–Tannmann–Hesse) behaviour, see Eq. (8), and the existence of a broad relaxation time spectrum:

$$\tau = \tau_0 \exp\left(\frac{B}{T - T_\infty}\right) \tag{8}$$

This analysis gives a final equation for the imaginary part as follows:

$$\theta''(T) = \left(\frac{\partial \theta'}{\partial T}\right)_\omega \frac{\pi (T - T_\infty)^2}{2B} \tag{9}$$

Therefore, the temperature dependence of $\theta''(T)$ at the different experimental frequencies can be estimated by substitution into Eq. (9) of the pair of T_∞ and B parameters, and also the derivative of the real part $\theta'(T)$.

The two conditions imposed in this semiempirical model for its application, are quite well satisfied by our compound. The segmental relaxation time follows VFTH behaviour, as one can see from the literature [16,17,29]. Taking into account these previous works and the further dielectric analysis performed from the dielectric measurement section, we have chosen the set of values $B = 665\,\mathrm{K}$ and $T_\infty = 265\,\mathrm{K}$, in Eq. (9). The results of $\theta''(T)$ so calculated indicate that the temperature of its maximum is practically insensible respect to the B and T_∞ chosen values. Only a small variation in the absolute value of the maximum is observed. Concerning the other condition, the smooth variation of the $\theta'(T)$, which can be realised in Fig. 3, indicates that a suitable broad distribution of relaxation times is present. The results of such calculations for $\theta''(T)$ are represented for the three frequencies by continuous lines in Fig. 3.

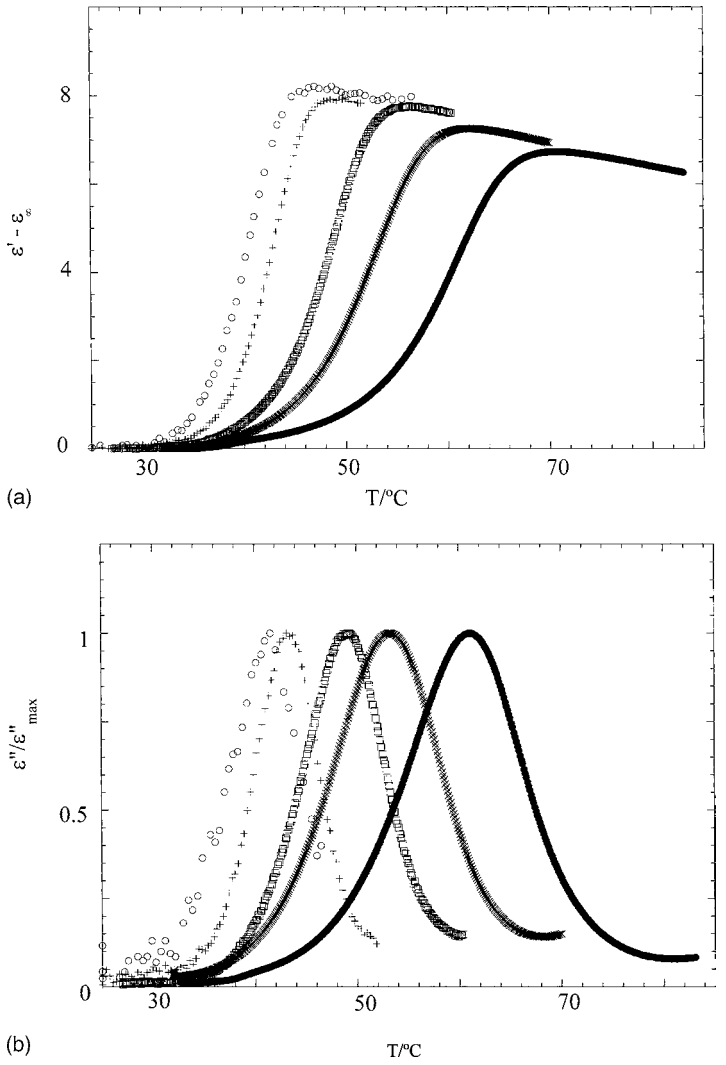

Fig. 4. Temperature dependence of the complex dielectric permitivity: (a) $\varepsilon' - \varepsilon_\infty$ and (b) ε''. Measurements have been performed at a scan rate of 4 K/h and at different frequencies: (○) 0.01 Hz; (+) 0.03 Hz; (□) 0.6 Hz; (×) 6 Hz; (●) 60 Hz.

3.2. Dielectric measurements

Significative differences between samples used by the different modulated calorimetric methods can invalidate the comparison which is one of our main objectives. In that sense, dielectric measurements have been performed for checking the quality of our PVAC sample (presence of water which acts as plasticisers, impurities, etc.). Two kind of dielectric measurements has been carried out.

A frequency sweep (0.7 Hz–1 MHz) was carried out under isothermal conditions at several temperatures above T_g, in the range from 45 to 105 °C. The results of the loss constant, ε'', indicate the presence of a conductivity contribution at low frequencies and an α process associated with the glass transition, whose effective relaxation time follows a VFTH behaviour. Due to the few experimental points with respect of the three parameters of the fitted function (B, $\log \omega_0$ and T_∞), the last one has been fixed to 265 K according to the reported data [16,17,27]. This parameter has been selected as fixed because it presents the lowest scatter between the reference sources. The fitted results give $B = 665 \pm 6$ K and $\log \omega_0 = 12.1 \pm 0.1$ rad s^{-1}, in good agreement with those reported in the previously mentioned references, supporting the quality of the sample. These parameters, as we have discussed above, have been used in order to evaluate the imaginary part of the dynamic heat capacity.

On the other hand, due to the fact that the TMDSC [17] and our calorimetric data correspond to isochronal data, dielectric measurements at the lowest possible scan rate (4 K/h) have been performed at different frequencies ($\nu = 0.01$, 0.03, 0.6, 6 and 60 Hz) and which also allow a comparison with the SHS results [16] obtained at high frequencies. The thermal dependence of both the dielectric constant, after subtracting ε_∞, and the loss constant are plotted in Fig. 4a and b, respectively, for the mentioned frequencies. The figures show the expected behaviour associated with the α process. In addition, the real part presents the influence of the thermal dependence of the static dielectric constant, ε_0, and the imaginary part shows the effect of the conductivity background.

In Fig. 5, the maximum of $\varepsilon''(T)$ and the frequency of the maximum of $\varepsilon''(\omega)$ are drawn in an activation plot together with the VFTH fits of the characteristic points obtained from the Beiner's [16] and Hensel's [17] isothermal dielectric data. The VFTH fit to our equivalent experimental data is also shown as a thick continuous line. Firstly, the results point out that a good agreement has been obtained between the deduced relaxation times from our isothermal dielectric spectra and those measured from the temperature of the maxima in our constant frequency series. On the other hand, although our isothermal data shows a small deviation respect to the Beiner's and Hensel's data, in the high frequency range, a good agreement appears at the low frequency range, where the main comparison between the calorimetric data will be done. This coincidence gives validity to our second goal which will be developed in the next section.

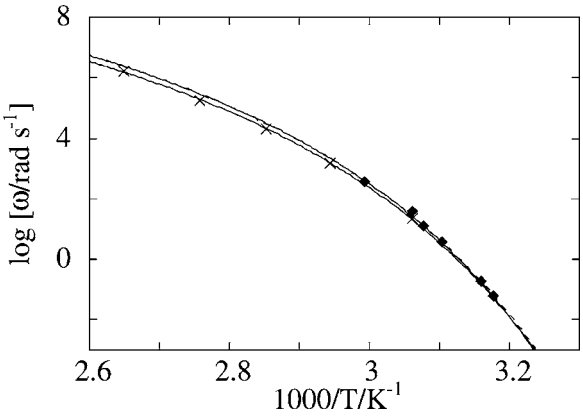

Fig. 5. Comparative activation plot for the dielectric measurements. (◆) Temperature of the $\varepsilon''_{max}(T)$ obtained from the experimental imaginary part plotted in Fig. 4(b); (×) frequency of the $\varepsilon''_{max}(\omega)$ obtained from the isothermal dielectric measurements; The thick continuous line is the VFTH fit to these last characteristic points. The thin continuous and dashed lines are the Beiner et al. [16] and Hensel et al. [17] VFTH fits, respectively.

3.3. Comparison between ac, SHS and TMDSC calorimetric data

The comparison between our calorimetric data and results coming from TMDSC [17] and SHS [16] have focused on two features: the width of the $\theta''(T)$ isochronal curve peaks and the values of the effective relaxation times deduced by two different methods. One from the maxima of the calculated $\theta''(T)$ and the other one from the step of $\theta'(T)$.

Concerning the widths, our calculated $\theta''(T)$ peaks yield values around 7 ± 1 °C at the 2–20 mHz

frequency range. The comparison with the TMDSC [17] data can be performed directly with the measurement corresponding to 40 mHz, which shows an imaginary part width of $8 \pm 1\,^{\circ}$C, very close to our experimental data. Besides, these values are also in agreement with those obtained from our isochronal dielectric measurements at the lowest frequencies, $\varepsilon''(T)$, $8.6 \pm 0.2\,^{\circ}$C. On the other hand, an increase in the width of the dielectric loss peak is observed when the frequency increases (see Fig. 4b). So, the width reaches $13\,^{\circ}$C when the frequency is increased to 60 Hz.

This tendency in the dielectric loss peak is in agreement with the SHS results which show a higher width of the heat capacity imaginary part in the frequency range 6–60 Hz. This behaviour has also been detected in the polystyrene (PS) [21,22] compound and has been associated to a decrease in the number of cooperatively coupled particles with increasing temperature. However in our case, a quantitative difference appears in the values of the width, since the values obtained using SHS are around $17\,^{\circ}$C at 60 Hz, while the dielectric one reaches only $13\,^{\circ}$C. At first glance, we must expect some differences due to the fact that we compare activities which sense differently the cooperative motions at the dynamic glass transition. Therefore, a possible interpretation of this additional broadening of the SHS loss peak could be the existence of relaxation modes which contribute to changes in the entropy, and carrying a very small dipole moment. However, when the comparison is made at the same temperature of $56.6\,^{\circ}$C between the dielectric $\varepsilon''(\omega)$ and the calorimetric spectra obtained by SHS, the widths are similar and even the calorimetric peak is 0.17 decades narrower than the dielectric one. Therefore, the hypothesis of the existence of extra modes must be discarded as an explanation for the SHS peak broadening in the isochronal calorimetric data.

In order to extend the analysis, let us to focus our attention to the PS sample. A careful comparison between the results [21,22] obtained by the same authors shows a large discrepancy between the width of the imaginary peak determined by SHS. Larger values are reported by Weyer et al. [21] which additionally do not fit well with the TMDSC data (differences of 3 K at the same dynamic glass transition temperature of 379 K), while recently Huth et al. [22] reports lower values (around 2–6 K lower than the Weyer data). In this case, the peak width obtained by both techniques (TMDSC and SHS) shows a good fitting. The authors indicate that the broadening of the dynamic glass transition is the main consequence of the developed stationary temperature field at the heater surface and in the surrounding. In this work, the problem was mainly resolved because the authors carefully followed an unified temperature calibration procedure for all the instruments [30] which, is based on the behaviour of a weak second order transition taking into account thermal lag effects due to the heating or cooling rate and the effects of the temperature amplitude on the heat capacity. In conclusion, we must suspect that the Beiner's SHS measurements can be influenced by this temperature profile throughout the sample inducing a broadening of the peak.

Furthermore, Weyer et al. [21] do not know exactly the reason for the temperature shift between the data from the SHS method and TMDSC measurements around 0.1 Hz when the relaxation times from both method are compared in the Arrhenius diagram. However, they suggest that the stationary temperature gradient may be also the reason for this shift. In order to proceed further with the comparison and to check if such effect is present on the PVAC SHS measurements, the comparison of the relaxation times is performed following the Arrhenius plot shown in Fig. 6. In the next analysis, we will take our dielectric results as reference, due to the good agreement with the data supplied by the different related works.

Our calorimetric data are represented by means of the temperature of the maximum obtained from the calculated $\theta''(T)$ and the half step height of $\theta'(T)$. Both characteristic points overlap within the temperature error bar, confirming the soundness of the used method to estimate the imaginary part. Quantitatively, a negative shift of approximately 0.2–0.3 frequency decades is observed from these data with respect to the dielectric one. The comparative analysis with the TMDSC [17] and SHS [16] data give also some differences. So, the frequency relaxation obtained by TMDSC shows a negative difference of around 0.4–0.5 decades with respect to the dielectric one, with the same tendency as our calorimetric data. In order to make a suitable comparison with the SHS results (half step height of $(\kappa C_p)'(T)$) carried out at high frequencies, we have performed an extrapolation of these data at the lowest frequencies, using a VFTH fit. The frequency

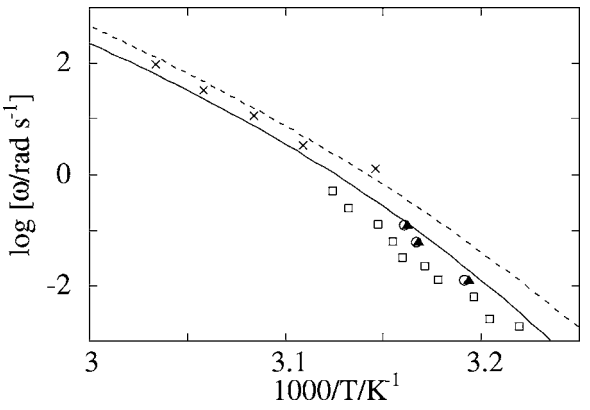

Fig. 6. Comparative Arrhenius plot showing the characteristic points of the different calorimetric techniques: (○) half step height of $\theta'(T)$; (▲) θ''_{max} obtained from the estimated imaginary part (Fig. 3); (×) half step height of the $(\kappa C_p)'$ from Beiner et al. [16]; (□) temperature of the maximum of $C''_p(T)$ obtained by TMDSC [17]. The continuous line represents the VFTH fit of our dielectric characteristic points obtained by the isothermal experiments. The dashed line is the reported VFTH fit to the SHS data of Beiner et al. [16].

relaxations so calculated undergo a positive difference of around 0.5 decades with respect to the dielectric data. This behaviour is in accordance with the data of Weyer et al. [21] for the PS sample. It means that the ac calorimetry and TMDSC techniques present a similar behaviour between them, clearly separate from the results of $(\kappa C_p)^*$ obtained by SHS where the effect of the stationary temperature field seems to be present.

On the other hand and in spite of the measurement of thermal conductivity on glasses show that this magnitude do not depend on frequency, recently and using a temperature wave technique [31], the thermal conductivity of the PVAC has been measured. The results show a frequency dependence in both the real and imaginary component of the magnitude κ^*. This complex behaviour complicates the analysis of the SHS data in order to obtain C_p^* because SHS measures the magnitude $(\kappa C_p)^*$, while ac calorimetry and TMDSC obtain directly C_p^*. In consequence, the temperature and frequency dependence of the thermal conductivity around the glass transition could also influence the results supplied by the SHS. However, these thermal conductivity data correspond to a PVAC sample with a different molecular weight and therefore a quantitative analysis cannot be performed.

Finally, both ac calorimetry and TMDSC data [17] show a negative shift of around one-third of the frequency decade with respect to dielectric spectroscopy data. This shift seems to be a quite general feature since it appears also for example in the well-studied glycerol system by SHS [11], where the frequency dependence of κ is negligible and both dielectric and SHS calorimetric measurements show similar loss peak widths in the $\varepsilon''(\omega)$ and $(\kappa C_p)''(\omega)$ spectra [32]. Additionally, this dielectric–calorimetric difference seems to be in agreement with the recent studies performed on PVAC, poly(bisphenol A, 2-hydroxypropyl-ether) (PH) and poly(vinyl methyl ether) (PVME) [33]. In this work, the enthalpy recovery of these compounds was investigated by using the DSC technique and the conclusion is that the structural relaxation time is about three times larger than the dielectric relaxation time in coincidence with our results.

4. Conclusions

Dynamic heat capacity measurements on PVAC in the region of the glass transition have been performed at very low frequencies using ac calorimetry. The temperature dependence of the real and imaginary part of $C_p^*(T)$, obtained by isochronal measurements close to a thermodynamic equilibrium, reflects the α relaxation process although the imaginary component is not well resolved. A semiempirical calculation of the imaginary part has been performed from a thermodynamic relationship between the real part, the frequency and the temperature, together with the Kramer–Kroning relationship for $C_p^*(\omega)$ and a Vogel–Fulcher–Tannman behaviour for the temperature dependence of the relaxation time. This mathematical procedure allows to estimate the temperature of the maximum of the heat capacity loss peak. The calculated width peak at very low frequency is in agreement with the TMDSC and dielectric data, but a discrepancy appears with the SHS measurements which show larger values. The calorimetric relaxation times that we observed are larger than the dielectric ones by about 0.3 frequency decades in agreement with TMDSC results but separated by about 0.5 in comparison to those obtained by SHS. The comparison with other systems seems to indicate that the thermal temperature gradient which can be

present in the SHS measurement can be the reason for the broadening and shift of the imaginary peak detected on the PVAC.

Acknowledgements

This work is dedicated to Prof. Domingo González, from the University of Zaragoza, on the occasion of his retirement.

References

[1] G.B. McKenna, S.C. Glotzer (Eds.), 40 Years of Entropy and The Glass Transition, J. Res. Natl. Inst. Stand. Technol. 102 (1997) (special issue).
[2] W. Kauzmann, J. Chem. Phys. 43 (1948) 219.
[3] A. Schönhals, F. Kremer, E. Schlosser, Phys. Rev. Lett. 67 (1991) 999.
[4] N. Menon, S.R. Nagel, Phys. Rev. Lett. 74 (1995) 1230.
[5] E.J. Leutheusser, Phys. Rev. A 29 (1984) 2765;
U. Bengtzelius, W. Götze, A. Sjölander, J. Phys. C 17 (1984) 5915.
[6] A.I. Mel'cuk, R.A. Ramos, H. Gould, W. Klein, R.D. Mountain, Phys. Rev. Lett. 75 (1995) 2522;
S.A. Kivelson, X. Zhao, D. Kivelson, Z. Nussinov, G. Tarjus, Physica A 219 (1995) 27;
S.A. Kivelson, X. Zhao, D. Kivelson, T.M. Fischer, C.M. Knobler, J. Chem. Phys. 101 (1994) 2391.
[7] N.O. Birge, P. Dixon, N. Menon, Thermochim. Acta 304/305 (1997) 51.
[8] T. Christensen, J. Phys. (Paris) Colloq. C8-635 (1985) 46.
[9] N.O. Birge, S.R. Nagel, Phys. Rev. Lett. 54 (1985) 2674;
N.O. Birge, S.R. Nagel, Rev. Sci. Instrum. 58 (1987) 1464.
[10] H. Gobrecht, K. Hamann, G. Willers, J. Phys. E 4 (1971) 21.
[11] N.O. Birge, Phys. Rev. B 34 (1986) 1631.
[12] Z. Kutnjak, C.W. Garland, Phys. Rev. E 55 (1997) 488.
[13] H. Yao, H. Nagamo, Y. Kawase, K. Ema, Biochim. Biophys. Acta 1212 (1994) 73.
[14] E. Freire, W.W. Van Osdol, O.L. Mayorga, J.M. Sanchez-Ruiz, Annu. Rev. Biophys. Chem. 19 (1990) 159.
[15] M. Settles, F. Post, D. Muller, A. Schulte, W. Doster, Biophys. Chem. 43 (1992) 107.
[16] M. Beiner, J. Korus, H. Lockwenz, K. Schröter, E. Donth, Macromolecules 29 (1996) 5183.
[17] A. Hensel, J. Dobbertin, J.E.K. Schawe, A. Boller, C. Schick, J. Therm. Anal. 46 (1996) 935.
[18] C. Schick, G.W.H. Hönne (Eds.), Temperature Modulated Calorimetry, Thermochim. Acta 304/305 (1997) (special issue).
[19] A.A. Minakov, Y.V. Bugoslavky, C. Schick, Thermochim. Acta 317 (1998) 117.
[20] S. Kahle, J. Korus, E. Hempel, R. Unger, S. Höring, K. Schröter, E. Donth, Macromolecules 30 (1997) 7214.
[21] S. Weyer, A. Hensel, J. Korus, E. Donth, C. Schick, Thermochim. Acta 304/305 (1997) 251.
[22] H. Huth, M. Beiner, S. Weyer, M. Merzlyakov, C. Schick, E. Donth, Thermochim. Acta 377 (2001) 113.
[23] S. Weyer, M. Merzlyakov, C. Schick, Thermochim. Acta 377 (2001) 85.
[24] U.G. Jonsson, O. Andersson, Meas. Sci. Technol. 9 (1998) 1873.
[25] S. Weyer, A. Hensel, C. Schick, Thermochim. Acta 304/305 (1997) 267.
[26] I. Hatta, A.J. Ikushima, Jpn. J. Appl. Phys. 20 (1981) 1995.
[27] J.A. Puértolas, M. Castro, I. Tellería, A. Alegría, J. Polym. Sci. B 37 (1999) 1337.
[28] M. Castro, J.A. Puértolas, J. Therm. Anal. 41 (1994) 1245.
[29] A. Alegría, E. Guerrica-Echevarria, L. Goitiandia, Y. Telleria, J. Colmenero, Macromolecules 28 (1995) 1516.
[30] C. Schick, U. Jonsson, T. Vassiliev, A. Minakov, J. Schawe, R. Scherrenberg, D. Lörinczy, Thermochim. Acta 347 (2000) 53.
[31] Y.I. Polikarpov, A.I. Slusker, Thermochim. Acta 304/305 (1997) 277.
[32] K.L. Ngai, R.W. Rendell, Phys. Rev. B 41 (1990) 754.
[33] A. Alegría, L. Goitiandía, Y. Tellería, J. Colmenero, Macromolecules 30 (1997) 3881.